

PEBB Thermal Management using ANSYS Multiphysics

Richard Garman

A&T Engineering Technologies, VECTOR Research Division

Annapolis, MD 21402-5067

ABSTRACT

Two-dimensional (2-D) computational fluid dynamic (CFD) and three-dimensional (3-D) heat transfer finite element analyses of various liquid heat sinks has been performed using ANSYS Multiphysics. This work is part of an effort funded by the Office of Naval Research (ONR) to characterize the thermal management of current and future heat dissipation devices used in the Power Electronic Building Blocks (PEBB) program. The PEBB modules are high power, compact, semiconductor devices. The typical footprint of a PEBB module baseplate is 16.7 square centimeters (cm^2) with a maximum power dissipation over 1400 watts.

Four water-flow heat sinks evaluated with ANSYS are presented in this paper. The baseline test case was an open-chambered heat sink with two inlet and two outlet flow connections. Two channel heat sink designs were modeled with different channel configurations. A diamond shaped post heat sink was also evaluated. The heat transfer analysis of each heat sink included a 2-D CFD model and a unique 3-D finite element analysis (FEA). This analytical work was conducted in parallel with laboratory testing.

ANSYS Multiphysics was used to correlate the test data with empirical relations and to develop the capability for scaling heat sinks for future PEBB designs. A thick film resistor (TFR) of approximately 12.5 ohms and 16.7 cm^2 in size was mounted in a PEBB housing and attached to the heat sink to simulate heat dissipation by a PEBB module. The CFD analysis calculated the velocity distribution through the heat sink at the interface with the TFR. The velocity distribution was used to calculate the nodal film coefficients, based on empirical relationships developed from the test data.

The average film coefficients were calculated in 2-D space in each model. A 3-D model of the TFR was developed to simulate the test heat source. The calculated array of film coefficients was applied to the bottom surface of the TFR model. A heat flux was applied to the top surface to represent the heat load. The solid model calculated the temperature distribution over the surface of the TFR. These values are compared to test measurements recorded with an infrared (IR) thermal imaging camera. The ANSYS contour plots do not provide an exact match with the IR camera temperature measurements, but the modeling data is within an acceptable range. The pressure drop across each heat sink was also calculated by ANSYS. These values are also within an acceptable range of the test measurements.

INTRODUCTION

VECTOR Research Division of Analysis and Technology (A&T) Engineering Technologies tested several liquid heat sinks for the Power Electronics Building Blocks (PEBB) program. This thermal management effort is part of a larger PEBB program sponsored by the Office of Naval Research (ONR). The PEBB program goal is to develop a high power multi-function power electronic device that can be reconfigured in situ via software programming. The drive to design small, lightweight power electronics has significantly increased the power density of these devices and has mandated the use of liquid cooling to dissipate the large heat fluxes.¹

The original PEBB heat sink module is a water-flow channel with pegs configuration. This heat sink bolts directly to the bottom of the PEBB module to allow direct contact of the water with the aluminum nitride baseplate. All tested heat sinks were attached to the test heat source in this manner. This PEBB heat sink was found to perform poorly in terms of both effectiveness and efficiency. The primary deficiency in effectiveness was the existence of hot spots due to areas of relatively stagnant flow. The poor efficiency of the heat sink manifests itself in the high water pressure drop across it.

A series of liquid heat sinks were developed to enhance the performance of the PEBB devices. Heat sinks are required to dissipate high heat fluxes while maintaining a low-pressure drop. VECTOR Research Division established a thermal baseline program to benchmark heat sink concepts. The thermal baseline program combined laboratory testing with analytical modeling. ANSYS Multiphysics was used as a tool in the analytical modeling effort to correlate the test data with analytical equations and to develop a means of scaling these and other heat sinks for future PEBB system designs.² This paper will discuss the test and analysis used to calculate the heat transfer properties of the various heat sinks and the modeling approach and results of this ANSYS modeling effort.

APPROACH

The PEBB thermal modeling and analysis was conducted in conjunction with the laboratory testing. The laboratory test conditions are the same boundary conditions and loads applied to the ANSYS models. Experimental data was required to develop accurate empirical equations to describe the relationship between the heat sink fluid dynamics and its ability to transfer heat to the working fluid. Test data used in the models include the pressure drop across the heat sink, the temperature at the surface of the heat source, and the applied heat flux.

The test heat source was 12.5-ohm, 16.7 cm², thick film resistor (TFR). Heat was generated by applying a voltage across the TFR. The electrical power produced simulated the heat losses in the PEBB devices. The TFR was printed on a 0.152 cm (0.06 in.) thick substrate made from 96% Alumina. The thermal conductivity of the Alumina substrate is a function of

temperature and is approximated by the linear expression shown as equation 1.^a The thermal conductivity of the substrate follows a slight power curve above a temperature of 100 °C, so this equation is only valid for test conditions between 10 and 100 °C.

$$k = -0.0008 \times T + 0.275 \quad (W/cm \cdot ^\circ C) \quad (1)$$

The pressure drop across each heat sink was recorded using two sets of gages. Dial gages were located at the inlet and outlet sides of the test apparatus. A differential pressure gage was also attached to the inlet and outlet ports of the heat sink, as a direct indicator of the pressure drop. Prior to testing a heat sink, the pressure drop across the test apparatus was calibrated to ensure the accuracy of the pressure measurements.

An infrared (IR) thermal imaging camera was used to record the temperature distribution on the top surface of the TFR. This temperature distribution was used to calculate the thermal impedance as shown in equation 2. The thermal impedance is the temperature differential required for a unit heat flux per unit area. Simply stated, the thermal impedance is the inverse of the convection (film) coefficient.² The thermal impedance provided a bridge between fluid dynamics and heat transfer performance.

$$\theta(x, y) = \frac{T(x, y) - T_\infty}{(q/A)_{\text{sink}}(x, y)} \quad (^\circ C - cm^2 / W) \quad (2)$$

The film coefficient or inverse of the thermal impedance is related to the fluid flow through the Nusselt number (Nu), as shown in equation 3. The Nusselt number is a function of the Reynolds number (Re) and the Prandtl number (Pr). The Prandtl number is simply a dimensionless parameter to describe the heat dissipation of a fluid relative to its momentum. The fluid flow regime mainly depends on the Reynolds number, which is the ratio of inertial forces to viscous forces. Empirical equations for the Nusselt number were determined from curve fits of the test data for each heat sink. These relationships, contained in table 1, were used to calculate a film coefficient at each node in the computational fluid dynamics (CFD) model.³

$$h = \frac{Nu * k}{L_c} \quad (W / cm^2 \cdot ^\circ C) \quad (3)$$

ANSYS Modeling

The ANSYS modeling approach was done in two stages. First, CFD models were developed for each heat sink. The CFD models calculated the pressure drop across the heat sink and the velocity profile through each heat sink. Next, three-dimensional (3-D) models were created to simulate the TFR. A constant heat flux and an array of film coefficients were applied to the TFR model to solve for the temperature degree-of-freedom (DOF).

^a Data received from Hybrid-Tek for TFR model Coors ADS-96R

Table 1. Empirical Nusselt Number Relationships

Heat Sink	Nusselt Number Equation
Open Chambered	$Nu = 0.845 * Re^{0.6127} * Pr^{1/3}$
Basic-Channeled	$Nu = 1.2199 * Re^{0.6126} * Pr^{1/3}$
30-Mil Diamond Post	$Nu = 0.623 * Re^{0.6166} * Pr^{1/3}$
Channeled with Pegs	$Nu = 2.6261 * Re^{0.8057} * Pr^{1/3}$

Separate 3-D models of the TFR were created for each heat sink analysis. The key to developing accurate TFR models is the proper construction and correlation of the nodal film coefficients calculated through the CFD velocity data. The TFR solid models are built from the two-dimensional (2-D) CFD meshed area models. The CFD models only represent the fluid flow chamber, so the internal rigid component areas (i.e., cutouts representing channel walls or posts) were reattached and meshed to provide a solid mesh of the TFR cross-sectional area. The 2-D mesh was then extruded by the thickness of the TFR. Before extruding the mesh, the element properties were set to change the element type from FLUID141 to SOLID70. For simplicity, the inlet and outlet ports modeled remained as 2-D elements, so the FLUID141 element was replaced with a SOLID55 element. Three or four element divisions were extruded in the z -direction depending on the size of the model.

The film coefficient data was stored in arrays with each array dimension relating to a particular node number. Separate macros were written for the CFD and finite element analysis (FEA) to handle the repetitive film coefficient calculations. The CFD macro dimensioned and stored the x and y velocity data into parameter arrays and saved this data to a file. The second macro, written for the solid model, first restored the x and y velocity array parameters. With the velocity data available, this macro then dimensioned the necessary arrays and performed the vector parameter functions required to calculate the film coefficients. The macro was slightly different for each TFR model since they each included the specific Nusselt number expression as shown in table 1. The film coefficient arrays were applied to the TFR models through the surface load function.

HEAT SINK MODELS

Four different PEBB heat sink models are described in this paper. The first model is a simple open-chambered device considered the PEBB thermal test baseline. Two other models are different channel approaches. The remaining model is an arrangement of diamond shaped posts. The four separate geometrical arrangements are described in this section and shown with their respective mesh. Table 2 is included to show the size of the eight separate models in terms of the number of nodes and elements.

Table 2. ANSYS CFD & FEA Model Sizes

Heat Sink Models	2-D CFD Analysis		3-D FEA	
	Nodes	Elements	Nodes	Elements
Open Chambered	5089	4880	21010	16400
Basic-Channeled	7183	6760	33532	24600
30-Mil Diamond Post	9268	8862	38080	28287
Channeled with Pegs	3665	3233	22470	17128

Open-Chambered Heat Sink

The baseline test case was an open-chambered device. This is a simple heat sink with two fluid inlet ports on one side and two fluid outlet ports on the opposite side. The hardware device is shown in figure 1. The dimensions of the fluid chamber are 5.21 cm (2.05 in.) in the longitudinal direction and 3.43 cm (1.35 in.) in the transverse direction. Each fluid port has an inside diameter (ID) of 0.444 cm (0.175 in.). Flow is assumed to enter each port in an equal proportion.



Figure 1. Open Chambered Heat Sink

The area model of this heat sink is shown in figure 2 with the mesh in figure 3. The area model was generated with rectangular boxes and the AGLUE command. The area model is the cross-sectioned slice at the centroid of the z-axis (height). The mesh was mapped with all quadrilateral elements with a finer grid near the walls of the device and along the flow path.

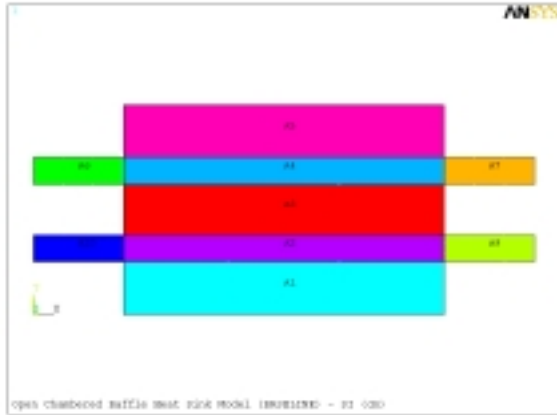


Figure 2. Open Chambered Heat Sink Area Model

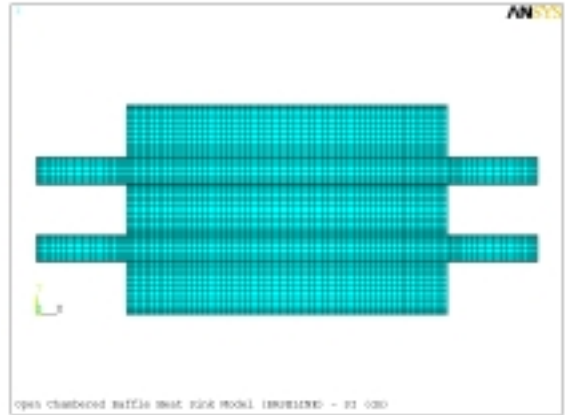


Figure 3. Open Chambered Heat Sink Meshed Model

Basic-Channel Heat Sink^b

The basic-channel heat sink consists of a single four-pass channel with the fluid entering and exiting the same side, as shown in figure 4. The fluid enters this device from the bottom; however, it is modeled as entering in the longitudinal direction. The overall length of the flow cavity in this model is 5.23 cm (2.06 in.) in the longitudinal direction and 3.38 cm (1.33 in.) in the transverse direction. The channel is 0.711 cm (0.28 in.) wide and a 0.178 cm (0.07 in.) solid wall separates each pass. The fluid inlet and outlet ID are each 0.635 cm (0.25 in.).

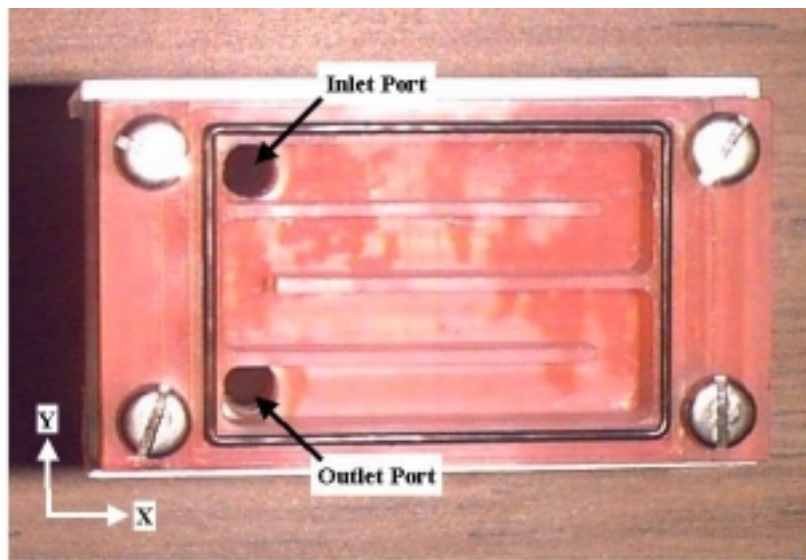


Figure 4. Basic-Channeled Heat Sink

^b This heat sink was designed and fabricated at VECTOR Research by machinist Pat Owens.

The area model is shown in figure 5 with the mesh in figure 6. This area model was also constructed with rectangular boxes and the AGLUE command. The inlet port is modeled as the left side of area 1 (A1) (see figure 5) with all the fluid entering along the longitudinal axis. The area model for this device is any cross-sectional slice perpendicular to the z -axis (height). Figure 6 shows the model's mapped mesh of quadrilateral elements.

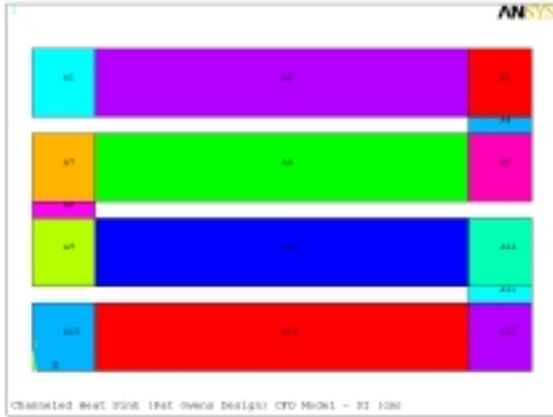


Figure 5. Basic Channeled Heat Sink Area Model

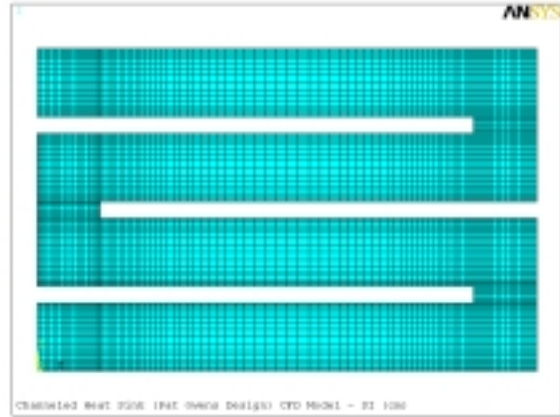


Figure 6. Basic Channeled Heat Sink Meshed Model

30-Mil Diamond Post Heat Sink

The 30-mil diamond shaped post heat sink consists of nine rows of 0.0762 cm (0.03 in.) high plastic posts arranged in a staggered array with seven posts per row. The fluid enters the bottom, as shown in figure 7, and exits the top. The flow length of this heat sink is 3.302 cm

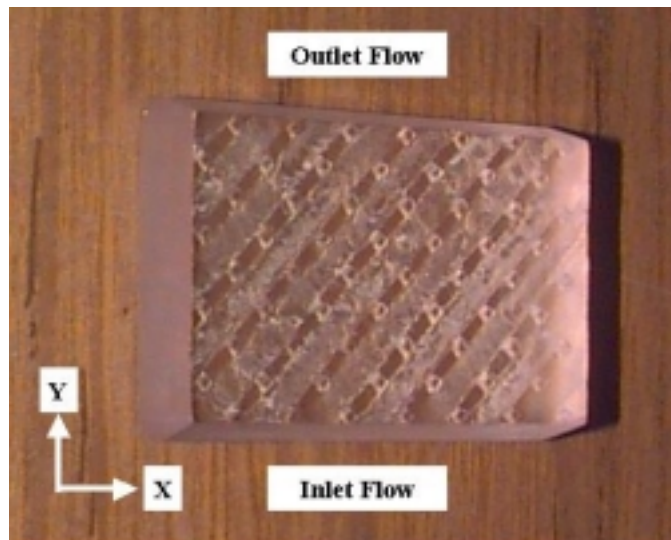


Figure 7. 30 Mil Diamond Posts Heat Sink

(1.33 in.) long and 5.05 cm (1.99 in.) wide. The fluid enters a specially designed manifold, via tubing, and the manifold directs the fluid through the diamond post passage between the heat sink and the TFR. The theory behind this design was to increase the fluid velocity and mixing to enhance turbulence.

The 30-mil diamond post area model is shown in figure 8 with the mesh in figure 9. The area model was generated by subtracting the 63 diamond post areas from the base area. The remaining area is irregular in shape and free meshed using quadrilateral elements. The mesh was partially controlled by specifying the number of element line divisions.

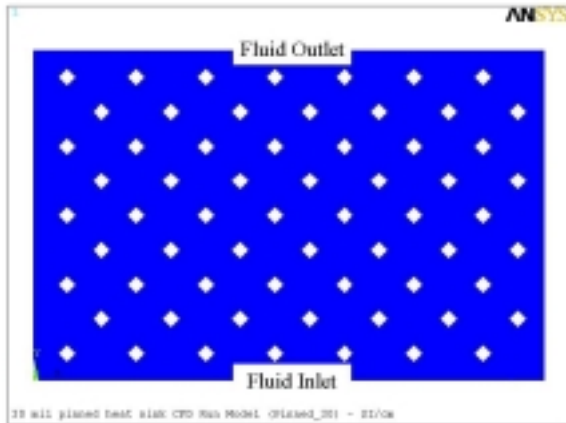


Figure 8. 30 Mil Diamond Post Heat Sink Area Model

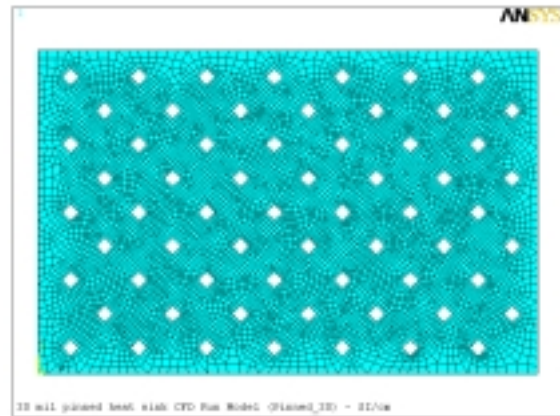


Figure 9. 30 Mil Diamond Post Heat Sink Meshed Model

Channeled Heat Sink with Pegs

The channeled heat sink with pegs is a modified version of the original PEBB heat sink. The original heat sink had a gap between the top surface of the channel and pegs and the PEBB baseplate to allow water flow over the top. This modified version raised the channel and pegs to

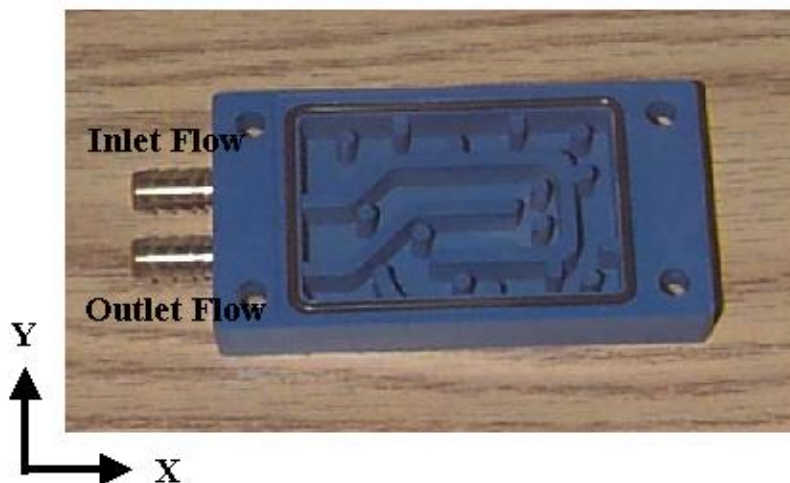


Figure 10. Channeled with Pegs Heat Sink

the baseplate, preventing the water from bypassing the flow channel. It consists of a single flow channel with the fluid entering and exiting the same side, as shown in figure 10. The fluid enters this device from the top port and exits from the lower port. The overall cavity dimensions are 5.21 cm (2.05 in.) in the horizontal direction and 3.43 cm (1.35 in.) in the vertical direction. The flow length of the channel is approximately 19.8 cm (7.78 in.). The channel width varies along the flow path with pegs placed in the flow regime to generate turbulence. The fluid inlet and outlet ID are each 0.444 cm (0.175 in.).

The area model of the channeled heat sink with pegs is shown in figure 11 and the mesh in figure 12. This model was generated by subtracting the 16 peg areas and the channel barriers from the base area. The remaining area is irregular in shape and meshed using free quadrilateral elements. The fluid ports were meshed using a mapped quadrilateral mesh.

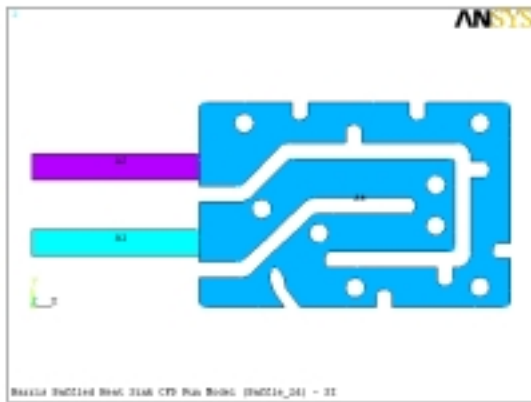


Figure 11. Channeled with Pegs Heat Sink CFD Area Model

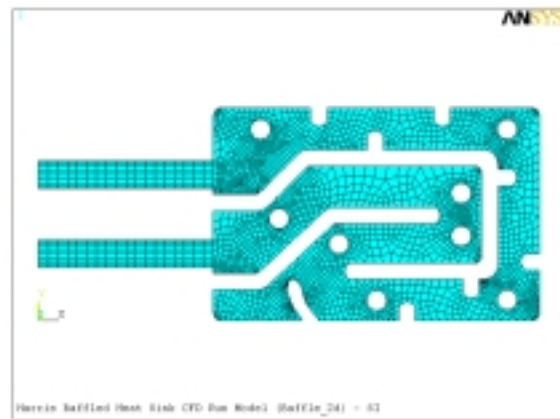


Figure 12. Channeled with Pegs Heat Sink CFD Meshed Model

MODEL SOLUTION

Achieving a valid CFD solution involved several steps. First, the fluid properties of water were input based on test conditions. Fluid density and viscosity are required for CFD analysis and were input in these analyses as constants. Solution stability was also considered. This included selecting the appropriate turbulent model and adjusting the relaxation factors. The standard κ - ϵ model, combined with a reduction in the relaxation factors, provided adequate convergence. After a solution reached the convergence termination criteria or the specified maximum number of iterations, the mass balance error was calculated to verify the solution satisfied the continuity equation. The temperature DOF solution of the FEA was more forthcoming.

Fluid Properties

All results contained in this paper are for a water flow rate of two gallons-per-minute (gpm) and a power dissipation of 600 Watts. The properties of water at the test conditions are shown in table 3. These properties of water are evaluated at the film temperature (i.e., the average contact temperature between the wall and the bulk fluid) which is described by equation 4. The TFR top surface temperature is corrected to the bottom surface temperature (T_w) in equation 4, based on the thermal conductivity of the substrate.⁴

$$T_f = \frac{T_w + T_\infty}{2} = \frac{\left[T_{res} - 0.68 \cdot \left(\frac{q}{A} \right) \right] + T_\infty}{2} \quad (4)$$

Table 3. Fluid Properties of Water

Heat Sink	Velocity (cm/s)	q/A (W/cm ²)	ρ (kg/cm ³)	k (W/cm-°C)	μ (kg/cm-s)	Pr
Open Chambered	406.6	36.29	9.943E-4	6.202E-3	7.415E-6	4.998
Basic-Channeled	398.4	35.76	9.962E-4	6.100E-3	8.543E-6	5.860
30-Mil Diamond Posts	327.6	35.82	9.965E-4	6.081E-3	8.776E-6	6.038
Channeled with Pegs	813.1	35.79	9.963E-4	6.0092E-3	8.643E-6	5.936

Stability

Reaching a valid convergence with the CFD models was difficult. Convergence of the pressure DOF was slow, requiring numerous iterations. Through necessity, the relaxation factor for the pressure DOF was reduced from a default value of 0.5 to values below 0.2. Convergence was verified when the mass balance satisfied the continuity equation. The mass balance was determined by comparing the average outlet velocity with the inlet boundary condition.

RESULTS

The results are presented in two parts. First, the ANSYS model pressure calculations are compared to the test data. The ANSYS pressure drop is calculated from the CFD pressure DOF solution at the inlet and outlet nodes. The second part compares the ANSYS temperature distributions with the thermal test images taken with the IR camera. The minimum, average, and maximum temperatures are also compared in tabular form.

Pressure Drop

Nodal DOF data calculated by ANSYS included the pressure. The ANSYS pressure drop was calculated by subtracting the average nodal outlet pressure from the average nodal inlet pressure. These values are shown in table 4 in both metric and English units. The ANSYS

calculated pressure contains the centimeter units for consistency with the model’s geometry and inlet velocity.

The percent errors between the ANSYS calculations and test data appear high. At further inspection, the values for the open-chambered, basic channeled, and 30-mil diamond post heat sinks seem reasonable for the 2-D fluid models. The hardware devices in all three of these models received some machining, leaving behind rough surfaces. This would increase the fluid friction and lead to higher test pressure readings. This would account for the high test pressure seen with the open channeled and 30-mil diamond post heat sinks. Both of these hardware devices have noticeable deposits left behind from the machining processes (see figures 1 and 7).

Table 4. Heat Sink Pressure Comparison

Heat Sink	ΔP_{test}		ΔP_{ANSYS}		Error (%)
	psi	kg/cm-s ²	Psi	kg/cm-s ²	
Open Chambered	2.25	155.1	1.08	74.54	-52.0
Basic Channeled	5.6	386.1	7.49	516.33	33.8
30-Mil Diamond Post	7.30	503.3	5.91	407.24	-19.0
Channeled with Pegs	12.10	834.3	52.4	3614.4	333.

The pressure calculated for the basic-channeled heat sink is higher than the measured value. This heat sink was cleanly machined which would lead one to believe that the modeled velocity was high, since pressure is a function of the velocity squared. A high velocity may be attributed to the fact that the model simulated the inlet velocity in the *x*-direction. In reality, fluid entered this heat sink from the *z*-direction. This assumption results in a higher modeled inlet velocity than under test conditions. The inlet velocity was also calculated from the area of the inlet port, instead of the channel cross-section. This also resulted in a higher modeled fluid inlet velocity.

The ANSYS calculated pressure drop across the channeled heat sink with pegs is over three times higher than the test measurements. Applying the above reasoning to explain this large variation does not fit. This would lead to the conclusion that the model was poorly constructed or meshed. The geometrical model appears to closely represent the hardware; therefore, the model’s mesh, shown in figure 12, probably needs some revision to improve accuracy.

Temperature Measurements

The temperature measurements are compared both visually and in tabular form. The IR cameral thermal images represent test data taken at the same conditions as the ANSYS solutions. Each of the thermal images contains many similarities to the ANSYS data. There are also a few differences of interest. Table 5 shows a tabular comparison of the two measurements. The test

values of interest are also shown on the thermal image. The ANSYS data was gathered by selecting only the surface nodes. The nodal results were listed for the temperature solution and sorted in descending order. The minimum and maximum values were easy to pick off this list. The average value was calculated by saving the nodal list and exporting the data to an Excel[®] spreadsheet.

Table 5. ANSYS vs. Test Data Temperature Comparison

Heat Sink	T_{\min} (°C)		T_{ave} (°C)		T_{\max} (°C)	
	Test	ANSYS	Test	ANSYS	Test	ANSYS
Open Channeled	59.5	34.6	69.9	60.2	84.3	87.3
Basic Channeled	44.5	40.7	58.8	46.0	70.7	64.1
30-Mil Diamond Post	46.9	49.5	54.8	51.3	58.5	55.2
Channeled with Pegs	48.1	37.8	57.0	44.4	76.7	82.0

Open-Chambered Heat Sink

Figures 13 and 14 show the thermal image of the open-chambered heat sink during testing and the ANSYS temperature solution, respectively. The ANSYS contour plot shows a symmetrical pattern not seen in the thermal image. This is attributed primarily to the cooling flow entering the test device. In ANSYS, it is very easy to apply an equal velocity to each inlet port. However, in the laboratory test environment, the thermal image moved as the inlet tubing was touched. The fittings used to split the flow also contribute to this error.

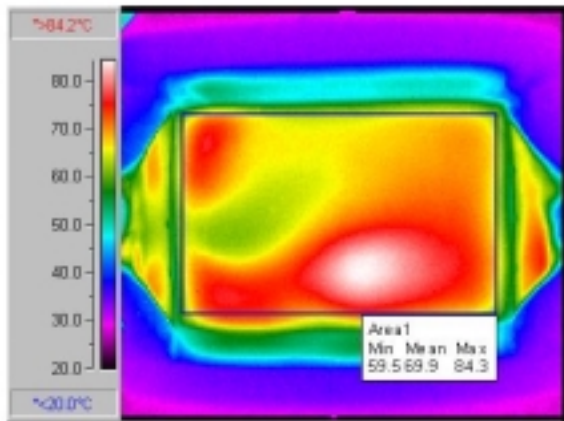


Figure 13. Open Chambered IR Thermal Image

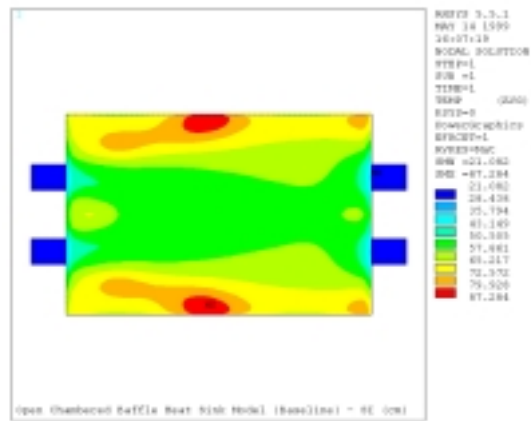


Figure 14. Open Chambered ANSYS Temperature Contour

The data contained in table 5 shows the ANSYS calculated temperatures are much lower than the test data. One contributing factor to these low ANSYS calculated temperatures is that the fluid temperature is held constant in the model. In the laboratory, only minor changes in the fluid bulk temperature are measure; however, the temperature change that occurs in the boundary layer increases significantly. The error in the maximum temperature, which is the primary quantity of interest, is only 3.5% higher, well within the accuracy of the test data.

Basic-Channeled Heat Sink

The images shown in figures 15 and 16 represent the test and ANSYS TFR temperatures recorded for the basic-channeled heat sink. The test image is oriented differently from the modeled image, as noted on each figure. The fluid inlet is at the lower right corner of figure 15 and the upper left corner of figure 16. In each image, the mixing generated at the corners enhances the cooling. The main difference between these temperature contours is that the flow field on the test image gets hotter as the fluid flows through the channels. This again is due to the temperature increases in the boundary layer of the test device, which is held constant in the ANSYS model.

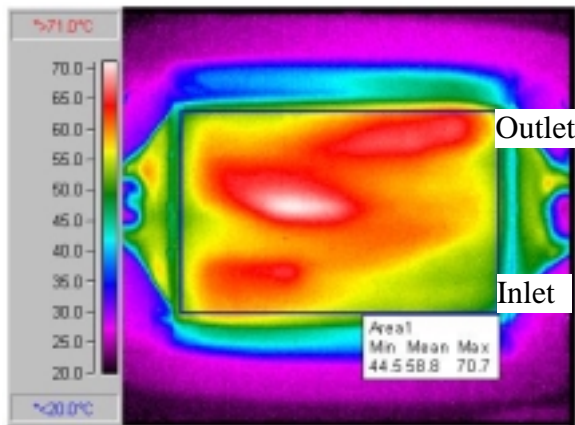


Figure 15. Basic-Channeled IR Thermal Image

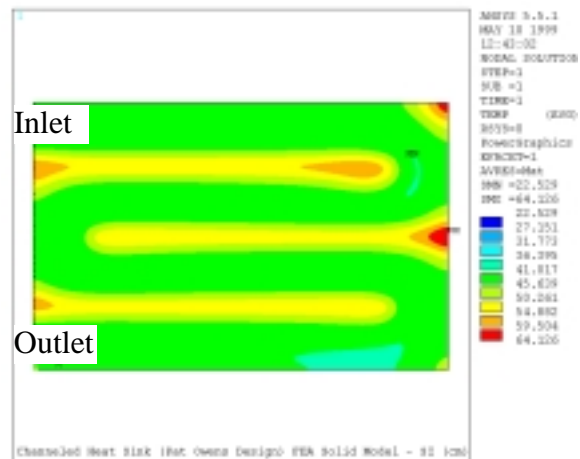


Figure 16. Basic-Channeled ANSYS Temperature Contour

A review of table 5 shows the minimum ANSYS temperature to be 8.5% lower than the measured temperature. The maximum and average surface temperatures have a similar error. Much of this is due to the model calculating and applying the film coefficient at a constant temperature. This model shows the need to vary the fluid temperature as a function of the boundary layer growth.

30-Mil Diamond Post Heat Sink

The temperature solution for the 30-mil diamond post heat sink provides a good match to the thermal test image (figure 17). Although the ANSYS contour plot in figure 18 does not

appear to be uniform, a close inspection of the figure shows only about a 3°C temperature difference between the red and yellow contours. These images show this heat sink to be very efficient and uniform. The red dots on the ANSYS contour are reflected on the test image as the white blurs, which are most noticeable at the leading and trailing edges.

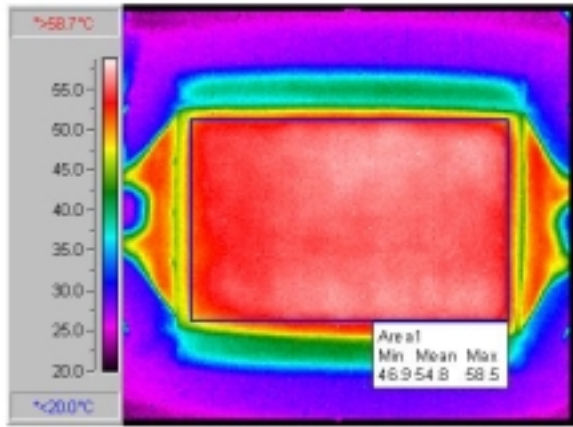


Figure 17. 30-Mil Diamond Post IR Thermal Image

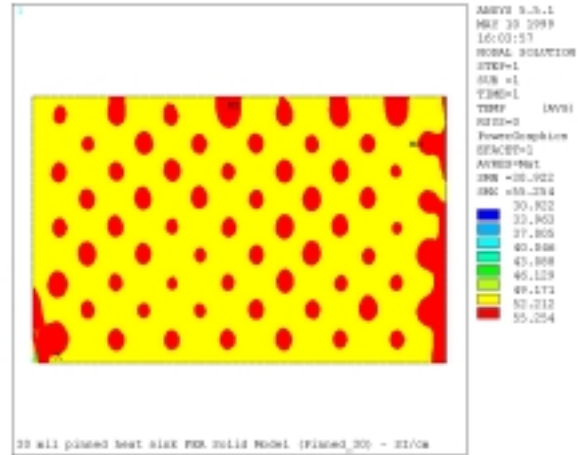


Figure 18. 30-Mil Diamond Post ANSYS Temperature Contour

The similar trend is shown in the tabular data. The ANSYS minimum temperature is about 5% above the test data, while the maximum ANSYS temperature is about 5% below the test data. The mean temperature error is also around 5%. This error is well within the experimental uncertainty.

Channeled Heat Sink with Pegs

The main item of interest in the solution for this heat sink is the location of the hot spot in the lower left corner, as shown in figure 19. The ANSYS solution in figure 20 shows the

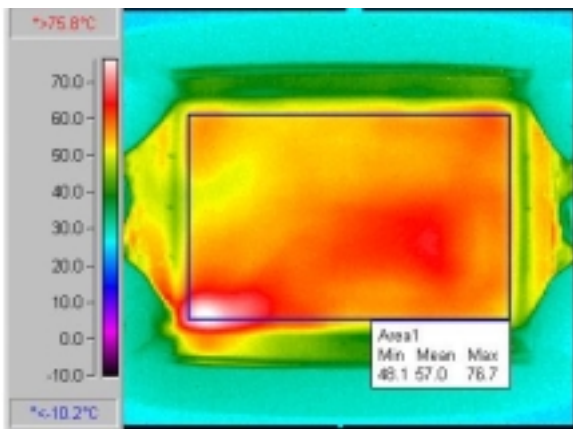


Figure 19. Channeled Heat Sink with Pegs IR Thermal Image

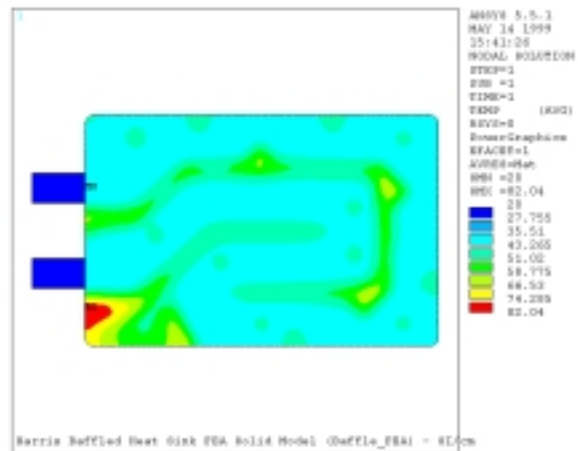


Figure 20. Channeled Heat Sink with Pegs ANSYS Temperature Contour

identical hot spot. The same fluid channel that appears faint on the thermal image is visible on both figures. Again, however, the thermal image gradual gets hotter through the channel due to the fluid temperature increasing as heat is transferred to the working fluid.

The ANSYS solution generated with this model an error range similar to the open chambered heat sink. The minimum temperature is significantly lower than the test data and the maximum temperature is moderately higher. The mean value is shifted to the low side accordingly. The mean and minimum calculated temperatures are within reason although they are 20% below the test data. The maximum temperature is acceptable at less than 7% error.

CONCLUSION

The ANSYS analysis agrees with the experimental data. The 30-mil diamond shaped post heat sink is both an efficient and effective heat sink for use in the PEBB program. The FEA solution shows a uniform surface temperature contour, which is very desirable in most heat sink applications. The low-pressure drop also makes this a more effective heat sink concept. Further modeling of this device could indicate optimal posts shapes and geometrical arrangements. A parametric modeling study would also indicate the most efficient post height.

ANSYS Multiphysics is shown to be an effective tool for calculating liquid heat sink performance by combining the CFD capabilities to calculate the film coefficient with the FEA capabilities to calculate device level heat abatement. A modeling capability has been developed which will provide a good qualitative analysis of numerous heat sink designs. This modeling capability can also be applied to analyze the effectiveness and efficiency of other PEBB program heat sink concepts, prior to machining and testing. ANSYS Multiphysics also provides a tool for parametric level studies of these devices for a full range of water flow rates and power levels. Various working fluids may also be qualitatively evaluated.

The value of experimental testing coupled with modeling has also been demonstrated. This was demonstrated using the empirical Nusselt number equations in table 1 to calculate film coefficients to generate valid temperature solutions to the solid model. These equations, derived from the test data, were the bridge connecting the 2-D CFD model velocity parameters to the 3-D FEA model temperature solution. Without valid test data, the film coefficients applied to the solid model would be inaccurate and produce meaningless results. In effect, the ANSYS modeling helped validate the experimental data by correlating these heat transfer calculations.

NOTATION

Acronyms

2-D	Two-dimensional
3-D	Three-dimensional
A&T	Analysis and Technology Engineering Technologies
CFD	Computational fluid dynamics
DOF	Degree-of-freedom
FEA	Finite element analysis
ID	Inside diameter
IR	Infrared
ONR	Office of Naval Research
PEBB	Power electronic building blocks
TFR	Thick film resistor

Units

cm	centimeter
gpm	gallons per minute
in.	inches
kg	kilogram
psi	pounds per square inch
s	second
W	watts
°C	degrees Celsius

Subscripts

ANSYS	ANSYS model data
ave	average
<i>f</i>	film
max	maximum
min	minimum
sink	heat sink interface
res	thick film resistor surface
test	test data
w	wall or fluid contact surface
:	free stream fluid conditions

Variables

h	convection (film) coefficient ($\text{W}/\text{cm}^2\text{-}^\circ\text{C}$)
k	thermal conductivity ($\text{W}/\text{cm-}^\circ\text{C}$)
L_c	characteristic length (cm)
μ	dynamic viscosity ($\text{kg}/\text{cm-s}$)
Nu	Nusselt number
Pr	Prandtl number
$q/A(x,y)$	heat flux per unit area (W/cm^2)
Re	Reynolds number
ρ	density (kg/cm^3)
T	temperature ($^\circ\text{C}$)
$T(x,y)$	local temperature ($^\circ\text{C}$)
θ	average thermal impedance ($^\circ\text{C-cm}^2/\text{W}$)
$\theta(x,y)$	local thermal impedance ($^\circ\text{C-cm}^2/\text{W}$)

REFERENCES

-
1. Terry Ericson, et al, "Standardized Power Switch System Modules (Power Electronic Building Blocks)," Office of Naval Research, White Paper (1997).
 2. Dr. Peter N. Harrison and Richard W. Garman, "PEBB Thermal Baseline Study Test Plan," A&T Engineering Technologies, VECTOR Research Division (July 8, 1998).
 3. Cengel, Yunus A., Heat Transfer: A Practical Approach, McGraw-Hill (1998).
 4. Dr. Peter N. Harrison and Richard W. Garman, "PEBB Thermal Management Final Report," A&T Engineering Technologies, VECTOR Research Division (May 1999).